BRL

AD

MEMORANDUM REPORT ARBRL-MR-02814

PROPOSED DESIGN FOR A DIFFERENTIAL PRESSURE GAGE TO MEASURE DYNAMIC PRESSURE IN BLAST WAVES

Noel H. Ethridge

March 1978

USA ARMAMENT RESEARCH AND DEVELOPMENT COMMAND
USA BALLISTIC RESEARCH LABORATORY
ABERDEEN PROVING GROUND, MARYLAND

Destroy this report when it is no longer needed.
Do not return it to the originator.

Secondary distribution of this report by originating or sponsoring activity is prohibited.

Additional copies of this report may be obtained from the National Technical Information Service, U.S. Department of Commerce, Springfield, Virginia 22161.

The findings in this report are not to be construed as an official Department of the Army position, unless so designated by other authorized documents.

The use of trade names or manufacturers' names in this report does not constitute indorsement of any commercial product.

REPORT DOCUMENTATION PAGE

READ INSTRUCTIONS BEFORE COMPLETING FORM

1. REPORT NUMBER: MEMORANDUM REPORT ARBRL-MR-02814
2. GOVT ACCESSION NO.:
3. RECIPIENT'S CATALOG NUMBER:

4. TITLE (and Subtitle): PROPOSED DESIGN FOR A DIFFERENTIAL PRESSURE GAGE TO MEASURE DYNAMIC PRESSURE IN BLAST WAVES

5. TYPE OF REPORT & PERIOD COVERED: Final

6. PERFORMING ORG. REPORT NUMBER:

7. AUTHOR(s): Noel H. Ethridge

8. CONTRACT OR GRANT NUMBER(s):

9. PERFORMING ORGANIZATION NAME AND ADDRESS:
US Army Ballistic Research Laboratory
(ATTN: DRDAR-BLT)
Aberdeen Proving Ground, MD 21005

10. PROGRAM ELEMENT, PROJECT, TASK AREA & WORK UNIT NUMBERS: RDT&E J11AAXSX352

11. CONTROLLING OFFICE NAME AND ADDRESS:
US Army Armament Research & Development Command
US Army Ballistic Research Laboratory
(ATTN: DRDAR-BL)
Aberdeen Proving Ground, MD 21005

12. REPORT DATE: MARCH 1978

13. NUMBER OF PAGES: 41

14. MONITORING AGENCY NAME & ADDRESS (if different from Controlling Office):
Defense Nuclear Agency
Washington, D.C. 20305

15. SECURITY CLASS. (of this report): UNCLASSIFIED

15a. DECLASSIFICATION/DOWNGRADING SCHEDULE:

16. DISTRIBUTION STATEMENT (of this Report):
Approved for public release; distribution unlimited.

17. DISTRIBUTION STATEMENT (of the abstract entered in Block 20, if different from Report):

18. SUPPLEMENTARY NOTES:

19. KEY WORDS (Continue on reverse side if necessary and identify by block number):
Dynamic Pressure Gage
Dynamic Pressure Measurements
Pressure Gage
Blast Wave Measurements
Air Flow Gage
Pressure Gage Diaphrams
Shock Tube Instrumentation
Blast Gage

20. ABSTRACT (Continue on reverse side if necessary and identify by block number) (mba)

The current technique for determining dynamic pressure in blast waves is subject to large errors below incident shock over pressures of 69 kPa (10 psi). It is shown that if a single pressure-sensing element can be used to measure the differential pressure between stagnation and side-on overpressures, then dynamic pressure can be determined with much less error. A design for a differential pressure gage is presented. A particular diaphram size and material are proposed, and several diaphram deflection-sensing techniques are indicated. The frequency response of the gage seems adequate for measurements

(Continued)

(Item 20 Continued)

of blast waves from large HE charges.

TABLE OF CONTENTS

LIST OF ILLUSTRATIONS

I. INTRODUCTION

The loading on a target produced by the blast wave from a large-scale explosion is usually described in terms of two phases. The diffraction phase occurs first and involves the phenomena produced when the shock front encounters and engulfs the target. The drag phase occurs after the rapid pressure variations associated with the diffraction process have ceased and a quasi-steady flow has been established over the target. The loading due to one or both phases may produce damage to the target, and therefore must be defined for calculating the response of the target or for correlating the response with previous test results.

On field experiments where targets are exposed to long-duration blast waves, overpressure as a function of time at the target or on the target can be recorded for use in determining the diffraction phase loading. Measurement of overpressure-time profiles at pressure levels of interest for military equipment can be performed satisfactorily using presently available instrumentation.

For determining drag phase loading on the target, the dynamic pressure is required as a function of time at the target location. The dynamic pressure is generated by the air flow occurring in the blast wave. Dynamic pressure currently is derived from separate measurements of stagnation overpressure and side-on overpressure versus time. Large errors in the determination of dynamic pressure may occur using the current technique at shock front overpressures less than 69 kPa (10 psi). Many critical items of Army equipment, such as communication systems, are damaged at incident blast overpressure levels less than 69 kPa (10 psi). The capability for making accurate measurements of dynamic pressure in the range of shock front overpressures as low as 21 kPa (3 psi) is required.

The purpose of this report is to present a design for a gage which offers the possibility of determining dynamic pressure versus time with satisfactory accuracy at such low incident blast overpressures.

II. CURRENT TECHNIQUE FOR DETERMINING DYNAMIC PRESSURE

The current technique for the determination of dynamic pressure in a blast wave involves the use of independent measurements of stagnation overpressure and side-on overpressure from gages which are physically separated, usually by several feet. The records from these gages are used to compute the dynamic pressure by use of fluid flow relations which are described, for example, in Reference 1. For this report only the subsonic flow regime is of interest, and the computational technique is described below.

---

[1] *H. W. Liepmann and A. Roshko, "Elements of Gasdynamics," John Wiley and Sons, Inc., New York, New York, 1957, p. 148-149. For derivation of dynamic pressure at a shock front, use equations on page 64.*

It is assumed that the fluid at the point of measurement experiences only isentropic changes. Then:

$$P_T = (P_s + P_A)\ [1 + (\gamma - 1)M^2/2]^{\gamma/(\gamma - 1)} - P_A \qquad (1)$$

where:

P_T = stagnation overpressure

P_s = side-on overpressure

P_A = ambient atmospheric pressure

γ = ratio of specific heats (assumed to be 1.4)

M = flow Mach number.

P_T and P_s are the quantities recorded by the stagnation and side-on overpressure gages used in field experiments.

Equation 1 is rearranged to provide M^2:

$$M^2 = [2/(\gamma - 1)] \left\{[(P_T + P_A)/(P_s + P_A)]^{(\gamma - 1)/\gamma} - 1\right\} . \qquad (2)$$

The dynamic pressure P_q is obtained from the overpressure value and the flow Mach number:

$$P_q = (\gamma/2)(P_s + P_A)M^2 \qquad (3)$$

where:

P_q = dynamic pressure = $1/2\ \rho\ u^2$

ρ = density

u = particle velocity.

When the value of M^2 from Equation 2 is substituted into Equation 3, dynamic pressure P_q can be expressed in terms of P_T and P_s:

$$P_q = [\gamma/(\gamma - 1)](P_s + P_A) \left\{[(P_T + P_A)/(P_s + P_A)]^{(\gamma - 1)/\gamma} - 1\right\}. \qquad (4)$$

The current technique for determining dynamic pressure in the subsonic flow regime is to insert the independently derived values of P_T and P_s into Equation 4 and calculate P_q.

At the blast wave shock front[1]:

$$P_q = P_s^2/[(\gamma - 1)P_s + 2\gamma P_A] = 2.5 P_s^2/(P_s + 7P_A) \text{ for } \gamma = 1.4 \qquad (5)$$

where the value of P_s is that for the incident peak overpressure.

If Equation 3 is solved for M^2 in terms of P_q and the result substituted into Equation 1, then:

$$P_T = (P_s + P_A)\left[1 + \frac{\gamma-1}{\gamma}\frac{P_q}{(P_s + P_A)}\right]^{\frac{\gamma}{\gamma-1}} - P_A . \qquad (6)$$

Using the value of P_q given by Equation 5 and $\gamma = 1.4$ in Equation 6, the value of P_T for shock front conditions is found to be:

$$P_T = (P_s + P_A)\left[1 + \frac{5}{7}\frac{P_s^2}{(P_s + P_A)(P_s + 7P_A)}\right]^{7/2} - P_A . \qquad (7)$$

For a given predicted incident shock front overpressure P_s, Equation 7 provides the corresponding value of P_T.

To obtain an indication of the error possible in P_q calculated using Equation 4 and independently measured values of P_T and P_s, calculations weremade for P_q under the assumption that the values of P_T and P_s had a maximum error of three percent. The particular values of P_T and P_s used were for shock front conditions, so that for a given incident shock overpressure P_s the corresponding value of P_T was calculated from Equation 7. The values of P_T and P_s were multiplied by the factors 1.03 and 0.97 and substituted into Equation 4. The maximum value of P_q was obtained for the combination of P_T three percent high and P_s three percent low, while the minimum value for P_q was obtained for P_T three percent low and P_s three percent high.

The percent error e in P_q was calculated as follows:

$$e = \frac{P_q' - P_q}{P_q} \times 100 \qquad (8)$$

where:

P'_q = $P_{q_{P_s}}$ calculated from Equation 4 using values of P_T and P_s, multiplied by 1.03 or 0.97 as indicated above.

P_q = value of P_q at shock front with peak overpressure of P_s, as calculated using Equation 5.

The results for e using the maximum three percent error in the values of P_T and P_s are shown in Figure 1. The value of P_A used was 101.325 kPa (14.696 psi).

Below about 100 kPa (14.5 psi) the error increases rapidly. At 69 kPa (10 psi) it is ± 28 percent, at 34.5 kPa (5 psi) it is ± 54 percent, and at 21 kPa (3 psi) the value is ± 87 percent. These values represent the error possible in determining the peak dynamic pressure assuming a maximum error of plus or minus three percent error in the measured values of P_T and P_s. In determining the dynamic pressure-time profile, the error will increase behind the shock front as the values of P_T and P_s decrease.

It is questionable whether the present instrumentation systems can provide pressure measurements in the field which have no more than three percent error, and it seems unlikely that a significant reduction below three percent can be achieved. Thus the current technique of determining dynamic pressure by using separate measurements of P_T and P_s is unsatisfactory for the lower overpressure levels of interest.

III. PROPOSED TECHNIQUE FOR DETERMINING DYNAMIC PRESSURE

The difficulty in the current technique of using independent measurements of stagnation overpressure and side-on overpressure to determine dynamic pressure is that at low side-on overpressures the errors in the measured signals may become as large or larger than the magnitude of the dynamic pressure. Thus the value of the differential pressure ($P_T - P_s$) calculated from independently measured values of P_T and P_s may be very much in error. However, if a sensing element can be used which will measure this differential pressure directly with no more error than occurs in the usual field pressure measurement, then dynamic pressure can be determined to about the same level of accuracy. At low overpressures this differential pressure is essentially equal to the dynamic pressure.

If Equation 4 is rearranged to express P_q in terms of the differential pressure D_q and P_s, the result is:

$$P_q = [\gamma/(\gamma - 1)](P_s + P_A)\left\{[1 + D_q/(P_s + P_A)]^{(\gamma - 1)/\gamma} - 1\right\} \quad (9)$$

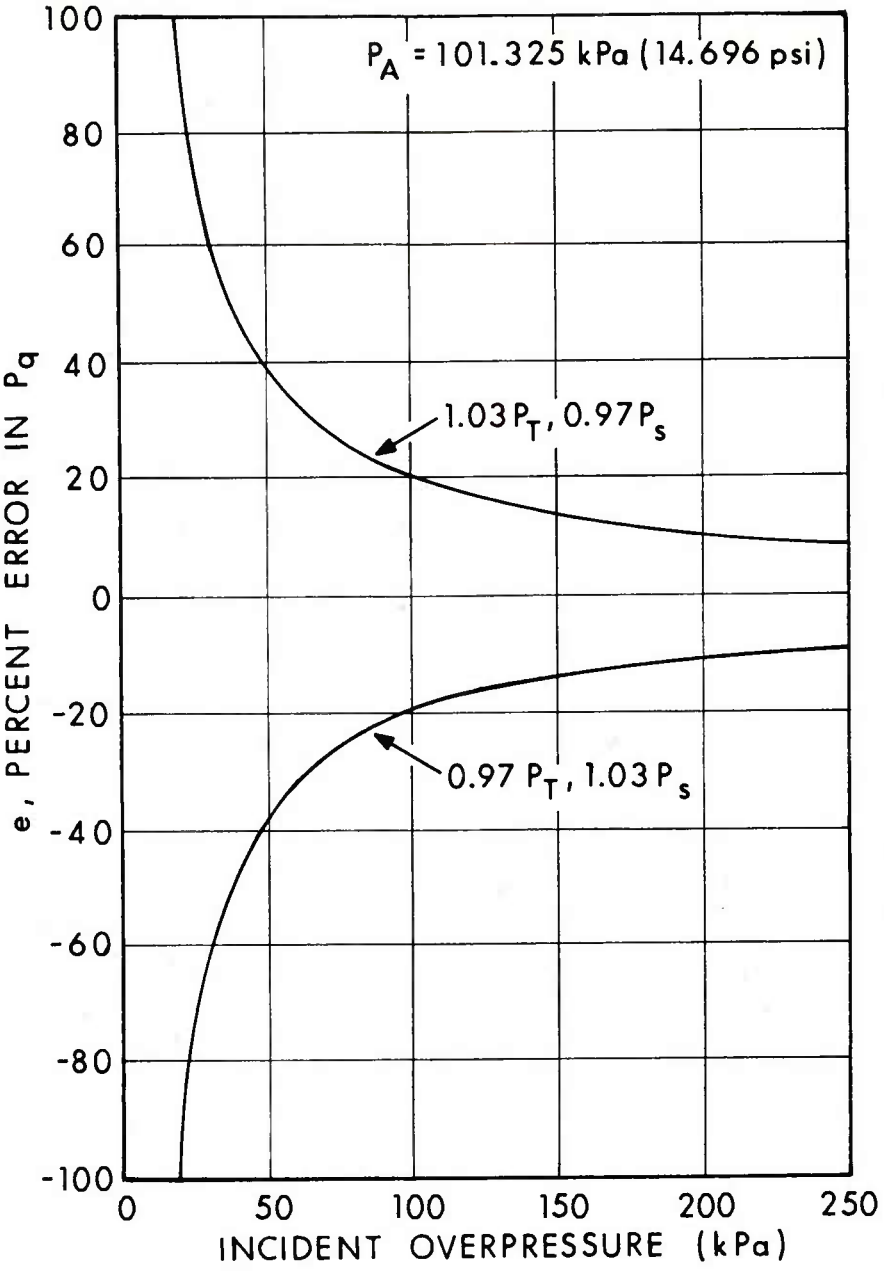

Figure 1 Maximum and minimum percent error in dynamic pressure versus shock front overpressure calculated using Equation 4 and the assumption of plus or minus three percent error in P_T and P_s.

where: $D_q = P_T - P_s$.

The proposed technique for determining dynamic pressure P_q is to use a gage designed to measure the differential pressure D_q versus time, another gage to measure overpressure P_s versus time, and then to calculate P_q versus time from these measured values using Equation 9. Because D_q is nearly equal to P_q at low overpressures, the change from the value of D_q produced by the use of Equation 9 is small, and is relatively insensitive to the value of P_s used.

The magnitude of the correction to the measured value of D_q to provide P_q is shown in Figure 2 by a plot of the ratio of P_q to D_q versus incident shock front overpressure. The solid curve is a plot of the ratio where D_q was calculated at shock front conditions. At incident shock overpressures less than 100 kPa (14.5 psi) the difference between P_q and D_q is less than five percent. Below 50 kPa (7.3 psi) incident shock front overpressure the correction to D_q to yield P_q generated by Equation 9 is less than two percent, and hence for this region the dynamic pressure can be directly equated to the measured value of D_q.

The dashed curves in Figure 2 show the variation in the ratio of P_q to D_q where D_q is unchanged from that used for calculating the solid curve but the value of P_s is changed by the factors 1.5 or 0.5. The results obtained from Equation 9 then correspond to using a correct value for D_q and a value for P_s with a large error. The dashed curves show that the ratio and hence P_q is changed by only a few percent at the lower overpressure levels, and thus the value of P_q calculated from Equation 9 is relatively insensitive to the value of P_s used. Normally on a field experiment a much more accurate record of overpressure versus time would be available for any station where dynamic pressure measurements were of interest.

In the proposed technique for determining dynamic pressure, then, the error in the dynamic pressure is essentially determined by the error in the measurement of D_q.

IV. PROPOSED GAGE DESIGN

The problem is to devise a gage to sense the differential pressure $P_T - P_s$ with reasonable accuracy (about five percent error) and adequate frequency response (zero to several thousand Hertz) suitable for use for measurements on HE blast experiments. The pressure-sensing element must respond to low differential pressures and yet have the required range of frequency response. The housing for the sensing element must minimize errors in pressure developed at pressure input ports. The entire gage must be as small as possible to minimize loss in frequency response due to long path lengths between pressure input ports and

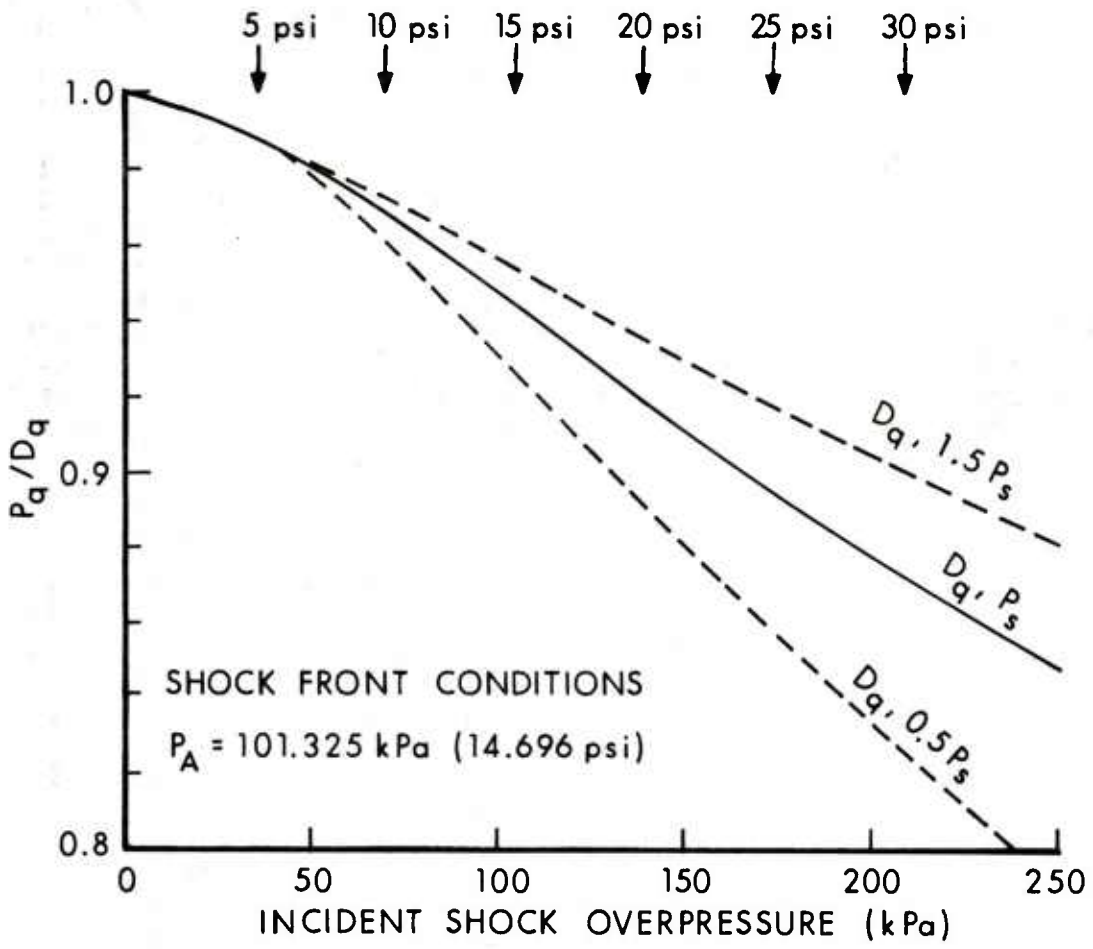

Figure 2 Ratio of dynamic pressure P_q to differential pressure D_q versus incident shock overpressure P_s. The dashed curves show the change produced by increasing or decreasing P_s used in Equation 9 by the factors 1.5 or 0.5, respectively.

the sensing element.

A proposed design for a differential pressure gage is shown in Figure 3. The outer configuration is that of a long cylindrical rod which is oriented parallel to the expected direction of air flow. The input pressure port for the stagnation overpressure is located in the nose of the rod, and is in the shape of a 15 degree half-angle cone. The apex of the cone occurs near the pressure-sensing diaphram. On the outside of the rod immediately behind the diaphram are located the input ports for the side-on overpressure. The ports are slots which provide an air path from the exterior atmosphere to a small cavity behind the diaphram. The slots extend around the circumference of the rod except for the minimum interruptions necessary to provide a metal connection between the forward and rear sections of the gage. The side-on pressure at these slots is lowered somewhat by the flow over the nose of such a gage configuration. This lowering of pressure at the slots is partially eliminated by rounding the edges of the slots. An additional increase can be produced by slightly enlarging the diameter of the rod at the rear edge of the slots. The inlet channels for both the stagnation and side-on pressures have right-angle direction changes so that dust particles in the blast wave cannot strike the diaphram directly. Some filter material is used in the channels to provide acoustic damping and to minimize the amount of dust which does penetrate into the cavities in front of and behind the diaphram.

The diaphram deflects according to the pressure difference developed between the cavities in front of and behind the diaphram, which should correspond to the differential pressure D_q. The diaphram movement can be detected by several techniques. In Reference 2 a variable-air-gap inductance type of sensing was used with success. The eddy current sensing technique such as is used in Kaman Sciences Corporation pressure gages may be satisfactory. Optical sensing of diaphram movement can be accomplished by using fiber optics to carry light to illuminate the diaphram and to collect and transmit reflected light to light sensors at some distance from the gages[3,4,5]. Reference 5 describes use of this technique with small-diameter (3-5mm) pressure gages. At least 0.1mm or so clearance should be provided between the diaphram and whatever

---

[2] *John L. Patterson, "A Miniature Electrical Pressure Gage Utilizing a Stretched Flat Diaphragm," NACA Technical Note 2659, 1952.*

[3] *R. Bailly-Salins, "Plastic Optical Fiber Displacement Sensor for Study of the Dynamic Response of a Solid Exposed to an Intense Pulsed Electron Beam," Rev. Sci. Instrum., Volume 46, No. 7, July 1975.*

[4] *J. Anthony Powell, "A Simple Two-Fiber Optical Displacement Sensor," Rev. Sci. Instrum., Volume 45, No. 2, February 1974.*

[5] *Gordon W. Margerum et al., "Fiber Optic and Laser Digital Pressure Transducers," Progress in Astronautics and Aeronautics, Volume 34, Instrumentation for Airbreathing Propulsion, 1974.*

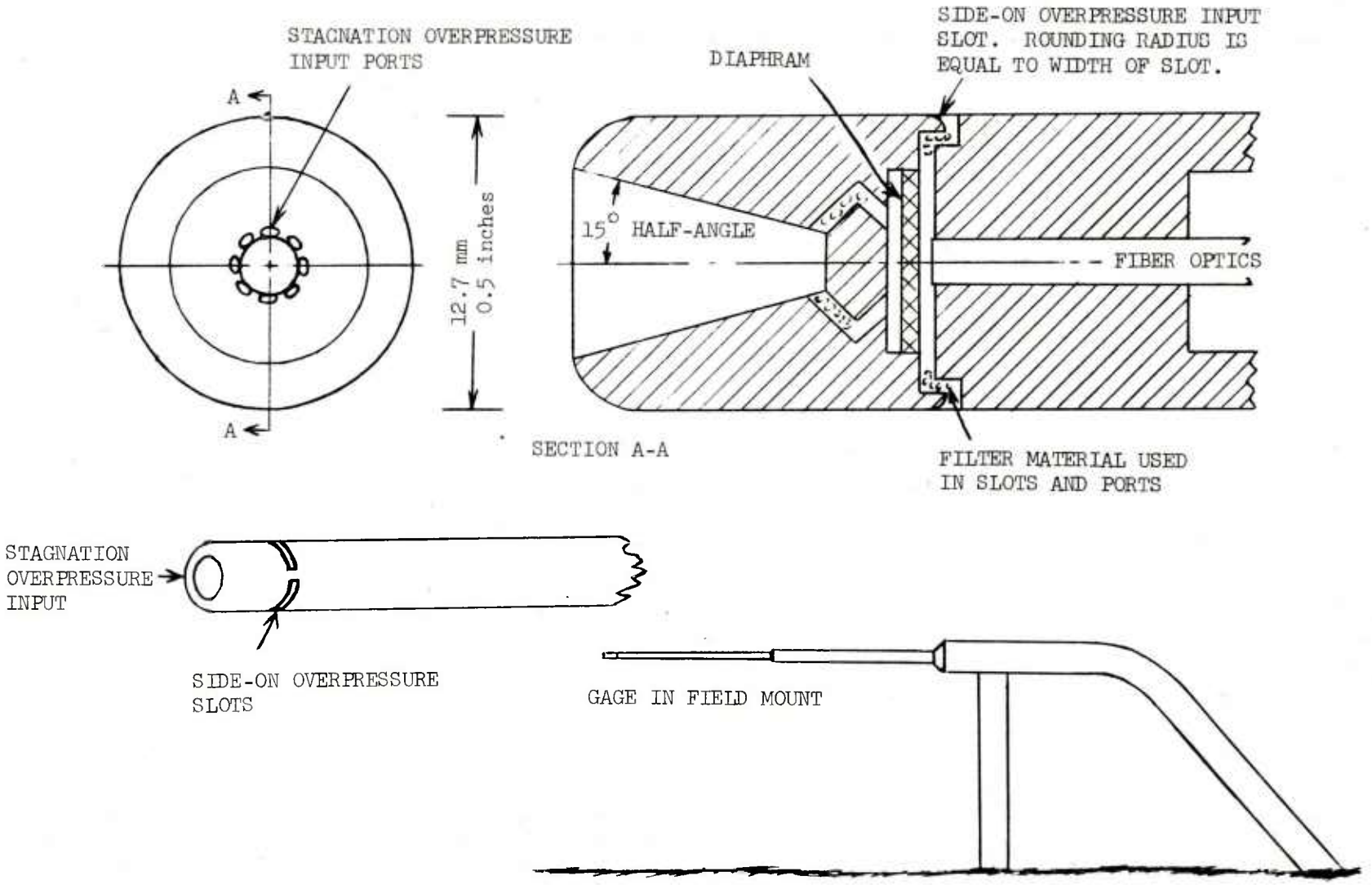

Figure 3 Proposed differential pressure gage design.

senses its motion, so that failure caused by dust particle jamming will be unlikely.

Further information which provided a basis for some of the gage features is presented in the following material, which is contained in Reference 6.

Figure 4 shows the variation in stagnation pressure versus angle of flow for different nose configurations. A cylinder with a 15 degree half-angle cone entrance is very insensitive to changes in flow angle. Although no configuration like that selected for the gage is shown, the curves for the other shapes in the figure suggest that the selected nose shape will produce an insensitivity to angle of attack over a range of about $\pm$ 20 degrees.

Figure 5 shows the variation in side-on pressure versus distance from the nose of the probe. At about 1.25 diameters to the rear of the nose the pressure is low by about three percent of the dynamic pressure. This lowering of pressure can be partially eliminated by modifying the pressure input opening used for the side-on overpressure. Figure 6 shows the effect of orifice edge form on pressure measurement in terms of percentage of dynamic pressure. If the edges are rounded with a radius equal to the diameter of the opening, the pressure developed in the port is increased by an amount equal to about one percent of the dynamic pressure. Although the information presented in Figure 6 is for cylindrical ports, a similar effect should occur for slots. The actual performance of the gage can be determined by placing it in known flows and establishing a correction factor to be used to convert the measured differential pressure to the true differential pressure.

The proposed diameter for the drilled holes used for stagnation pressure inlets is the same as that currently used on blast pressure gages, i.e., 1.016mm (0.04 inches) in diameter. The slots would be of this width also.

The proposed pressure-sensing diaphram is a stretched diaphram of the same material as its mounting, to minimize variations in diaphram tension caused by differences in thermal expansion characteristics between diaphram and mounting. The diaphram is placed under initial tension to increase the fundamental frequency and to minimize the effects of irregularities in thin diaphram materials.

Ideally, a very small diaphram would be used, so small that the fundamental frequencies would be high enough that no initial tension would be required for an adequate range of frequency response, and so that gage diameter and hence acoustic resonance frequencies would be as high as possible. However, the smaller the diaphram, the smaller

---

[6] *R. P. Benedict, "Fundamentals of Temperature, Pressure, and Flow Measurements," John Wiley and Sons, Inc., New York, N. Y., 1969.*

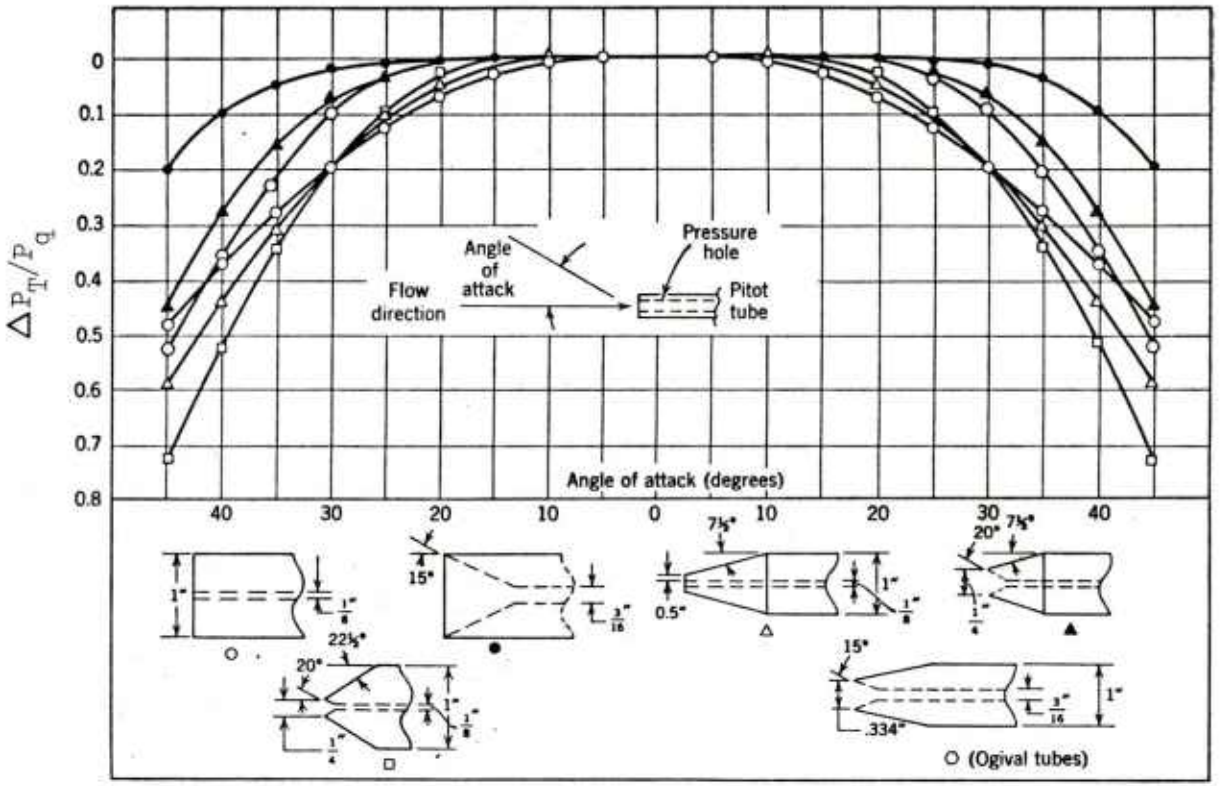

Figure 4 Variation of stagnation pressure indication with angle of attack and geometry for Pitot tubes, from Reference 6.

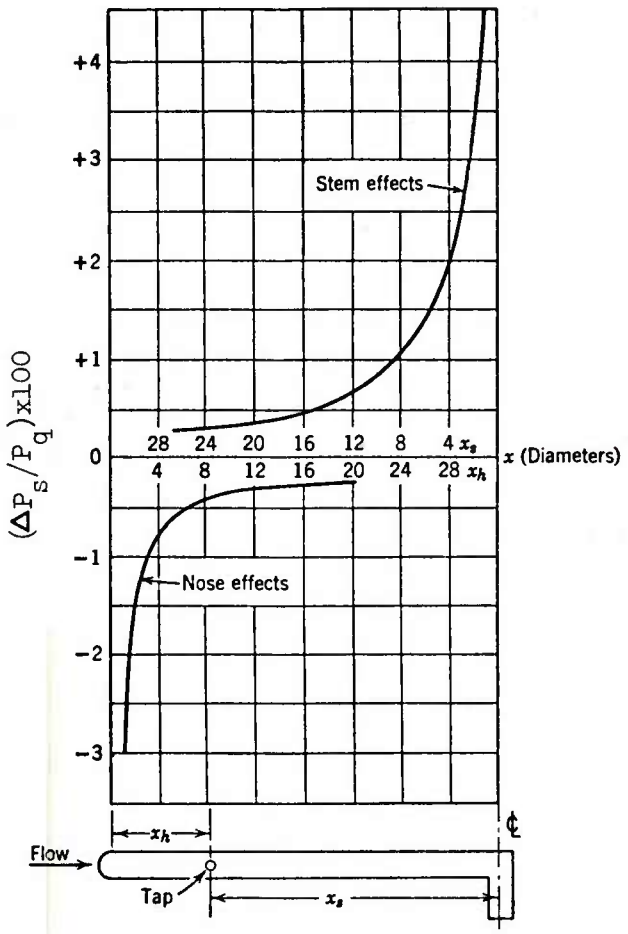

Figure 5 Nose and stem effects on side-on overpressure measurements along a static pressure tube, from Reference 6.

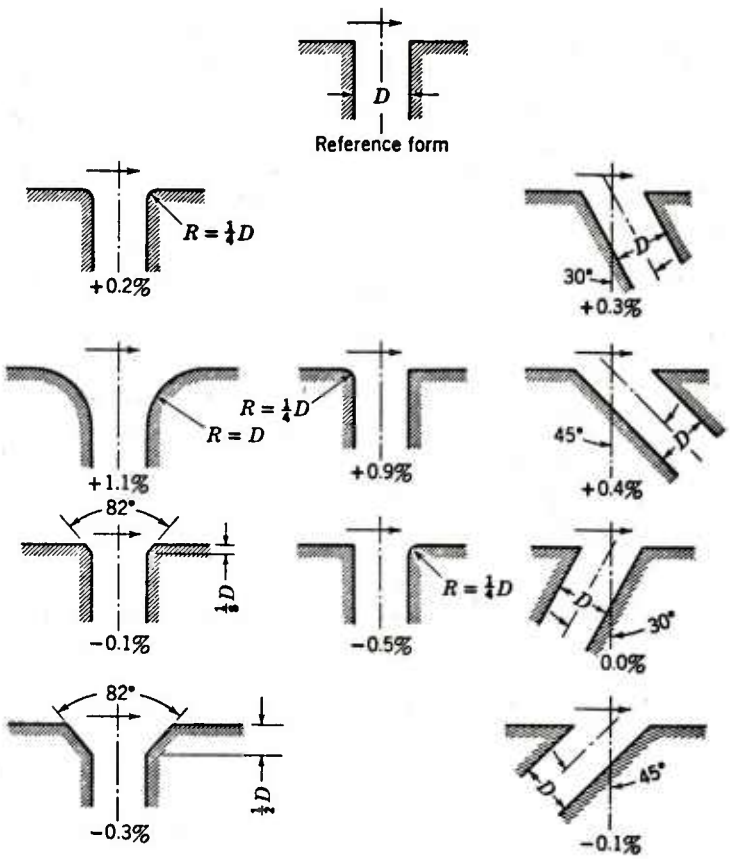

Figure 6 Effect of orifice edge form on side-on pressure measurement, from Reference 6. The variation is listed in percentage of dynamic pressure.

the deflection to be sensed, and hence obtaining a useful signal from the gage becomes more difficult.

An initial proposed diaphram is of a nickel-iron alloy that was successfully used in the NACA miniature electrical pressure gage Model 49, designed by the Instrument Research Division of the Langley Aeronautical Laboratory[2]. Model 49 gages were constructed to measure maximum pressures as low as 3.45 kPa (0.5 psi) and as high as 689 kPa (100 psi). The design process and construction details, including the technique used to produce the stretched diaphrams, are contained in Reference 2. The diaphram diameter used in the Model 49 gage was 7.94 mm (5/16 inches) in diameter. The equations used in calculating the properties of such a diaphram in the material that follows were taken from Reference 2.

The maximum diaphram deflection of the lowest range Model 49 gage (3.45 kPa or 0.5 psi) was about 0.0081 mm (0.00032 inches). Thus a peak full scale deflection of 0.01mm (0.00039 inches) seems a reasonable minimum deflection to require for an adequate output from a deflection-sensing technique. If the peak deflection is fixed at this value, the corresponding required initial diaphram tension and resulting fundamental frequency can be calculated for various peak pressures of interest.

The diaphram is assumed to be a flat stretched circular diaphram having its edges completely fixed. It is also assumed that the following relations hold:

$$w < 8T$$

$$s_o < 10t^2/R^2$$

where:

w = deflection of diaphram at center

t = diaphram thickness

R = diaphram radius

s_o = strain due to initial diaphram tension.

Then:

$$D_q = \frac{16}{3} \frac{E t^3 w}{(1 - \sigma^2)R^4} \left[1 + \frac{5(1 + \sigma)}{6} s_o \frac{R^2}{t^2} + \frac{(1 + \sigma)(173-73\sigma)}{360} \frac{w^2}{t^2}\right] \quad (10)$$

where:

D_q = differential pressure

E = Young's Modulus of elasticity

σ = Poisson's ratio.

A range of differential pressures corresponding to incident side-on overpressures were calculated. For these pressures and the diaphram thicknesses listed in Reference 2 and for a peak deflection of 0.01 mm, the initial strains s_o were calculated by solving Equation 10 for s_o as follows:

$$s_o = \frac{9(1 - \sigma)R^2}{40\ E\ w\ t} D_q - \frac{6t^2}{5(1 + \sigma)R^2} - \frac{(173-73\sigma)w^2}{300\ R^2} . \qquad (11)$$

The values obtained for s_o are shown in Table I, where the parameter values used were as follows:

R = 3.969 mm (5/32 inches)

E = 1.517×10^8 kPa (22×10^6 psi) for 42 percent nickel and 58 percent iron alloy

σ = 0.29

w = 0.01mm (0.0003937 inches).

The non-linearity of the deflection versus pressure curve is indicated by the ratio R_N of the last term in the brackets of Equation 10 to the other terms in the bracket:

$$R_N = \frac{(1 + \sigma)(173 - 73\sigma)\ w^2}{360\ t^2 + 300(1 + \sigma)\ s_o R^2} . \qquad (12)$$

The percent non-linearity, then, is:

$$P_N = 100\ R_N \qquad (13)$$

The percent non-linearity calculated for pressures of interest is listed in Table I also.

A graphical solution for the fundamental frequencies of a stretched diaphram is contained in Reference 2. The result is utilized below.

Table I. Diaphram Properties for Various Peak Overpressures for a Peak Deflection of 0.01 mm (0.0003937 inches)

P_s		P_T		P_q		D_q		t		s_o	F_1	F_2	Hz	P_N
(kPa)	(psi)	(kPa)	(psi)	(kPa)	(psi)	(kPa)	(psi)	(mm)	(in)	(mm/mm)				
20.68	3	22.16	3.21	1.465	0.213	1.471	0.213	0.0254	0.001	0.00055	14.70	14.3	4820	3.5
34.47	5	38.51	5.59	3.995	0.579	4.037	0.586	0.0254	0.001	0.00022	59.57	22.4	7550	1.2
48.26	7	56.09	8.14	7.687	1.115	7.829	1.136	0.0254	0.001	0.00047	126.12	30.3	10210	0.63
50.33	7.3	58.83	8.53	8.337	1.209	8.503	1.233	0.0254	0.001	0.00051	137.92	31.6	10650	0.58
55.16	8	65.34	9.48	9.950	1.443	10.18	1.476	0.0381	0.0015	0.00035	42.22	19.8	9990	0.73
68.95	10	84.71	12.29	15.27	2.215	15.77	2.287	0.0381	0.0015	0.00060	71.32	24.0	12140	0.47
103.4	15	138.3	20.05	32.90	4.772	34.83	5.052	0.0762	0.003	0.00041	12.28	13.9	14060	0.43
137.9	20	198.9	28.84	56.11	8.139	60.97	8.843	0.1016	0.004	0.00038	6.42	12.2	16450	0.32
172.4	25	266.3	38.62	84.25	12.219	93.92	13.622	0.1016	0.004	0.00092	15.45	14.6	19700	0.21
206.8	30	340.3	49.35	116.8	16.934	133.4	19.351	0.1422	0.0056	0.00036	3.06	11.3	21300	0.21
241.3	35	420.5	60.99	153.2	22.213	179.2	25.989	0.1422	0.0056	0.00089	7.63	12.6	23800	0.15
275.8	40	506.7	73.50	193.0	27.997	230.9	33.496	0.1803	0.0071	0.00020	1.06	10.5	25130	0.15
310.3	45	598.7	86.83	236.0	34.236	288.4	41.834	0.1803	0.0071	0.00073	3.88	11.5	27500	0.12
344.7	50	696.1	100.96	281.9	40.884	351.4	50.963	0.1803	0.0071	0.00131	6.97	12.3	29440	0.10

Figure 7 shows a plot of F_2 versus F_1; where:

$$F_1 = 12\ R^2\ s_o\ (1 - \sigma^2)/t^2$$

$$F_2 = 2\ R^2\ \omega_m \sqrt{3\ \rho_d (1 - \sigma^2)}/(t\ \sqrt{Eg}) \tag{14}$$

where:

ω_m = mechanical fundamental frequency of diaphram, radians/second

g = acceleration due to gravity

ρ_d = density of diaphram material (8000 kg/m^3 or 0.289 lbf/in^3).

To obtain the fundamental frequency F_1 is calculated, and F_2 is read from the curve in Figure 7. Then from Equation 14:

$$\omega_m = F_2\ t\ \sqrt{Eg}/\left[2\ R^2 \sqrt{3\ \rho_d\ (1 - \sigma^2)}\right] \tag{15}$$

and

$$f = t\ \sqrt{Eg}\ F_2/\left[4\pi R^2 \sqrt{3\ \rho_d\ (1 - \sigma^2)}\right] \tag{16}$$

where f is in Hertz.

Values of F_1, F_2 and f are listed in Table I.

The amount of non-linearity and the magnitude of the fundamental frequency seem adequate for gages to be used on large explosions. The only non-linearity significantly greater than one percent is for the diaphram used at the lowest pressure listed. This non-linearity can be reduced if the diaphram sensing technique operates satisfactorily with a peak diaphram deflection less than 0.01 mm.

The acoustic resonance frequency is difficult to calculate accurately for the proposed gage configuration. Considering the conical stagnation pressure inlet as a closed end tube, a value of about 9000 Hz is obtained for the lowest pressure of interest. The acoustic resonance frequency for the gage may well fall near the fundamental frequency of the diaphram, and hence the use of acoustical damping may be necessary to avoid undesirable ringing.

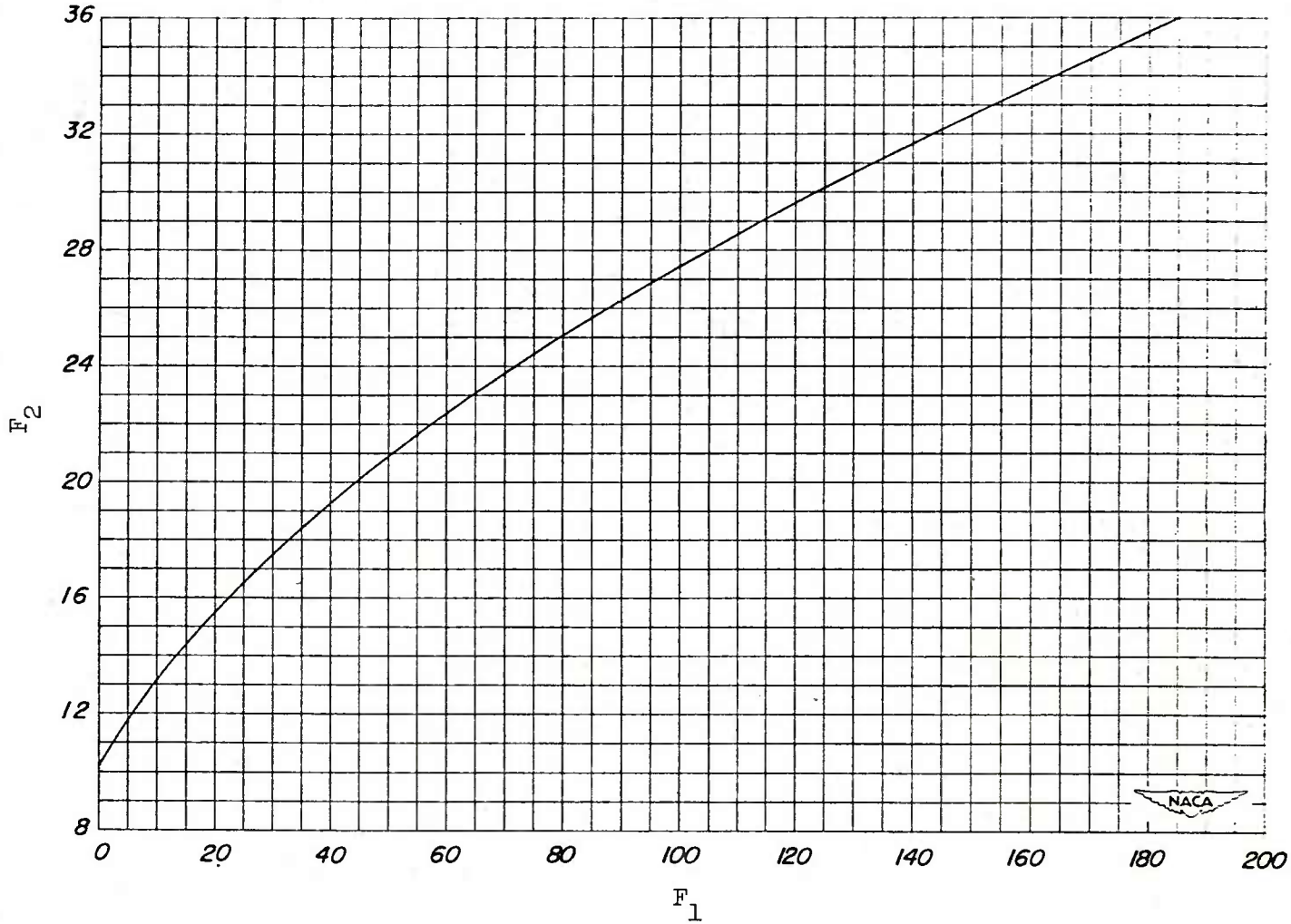

Figure 7 Graphical solution for the fundamental frequency of any clamped, circular, flat diaphram under radial tension, from Reference 2.

V. SUMMARY

The inadequacy of the current technique for determining dynamic pressure at low incident shock side-on overpressures was demonstrated by presenting the possible error which may occur by use of independent stagnation and side-on overpressure measurements with an error of three percent. No substantial reduction in the resulting large error in the dynamic pressure seems possible using this technique.

It was shown that if a single pressure-sensing element can be used to determine the differential pressure between the stagnation and side-on overpressures, then this difference pressure is essentially equal to the dynamic pressure at the lowest side-on overpressures of interest, and that at higher pressures the correction needed is small, so that the error in the dynamic pressure is essentially determined by the error in the differential pressure measurement. The possibility of measuring this pressure with an error no larger than about plus or minus five percent seems reasonable.

A design for a differential pressure gage was developed which seems workable without requiring new technical developments. A particular diaphram size and material are proposed based on their previous successful use in a family of pressure gages. The design may be further improved for higher frequency response by using smaller diaphrams. However, some experimentation with diaphram materials and deflection-sensing techniques may be required to achieve a significant reduction in gage size.

The proposed gage, if it performs as expected, will provide measurements of dynamic pressure of satisfactory accuracy in the blast overpressure regime of particular interest for critical items of Army equipment.

ACKNOWLEDGEMENT

The leading edges of the conical stagnation pressure inlet were rounded at the suggestion of Dr. Ray Sedney of the BRL in order to promote smooth flow over the side-on pressure inlet slots.

LIST OF SYMBOLS

e	percent error in P_q
f	fundamental frequency of diaphram, Hertz
g	acceleration due to gravity, m/s^2
s_o	strain in diaphram due to initial diaphram tension, mm/mm
t	diaphram thickness, mm
u	particle velocity, m/s
w	deflection of diaphram at center, mm
x	diameter of a static pressure tube, m
x_h	position of taps from base of nose of a static pressure tube, m
x_s	position of taps from center line of stem on a static pressure tube, m
D	diameter of a pressure orifice, mm
D_q	differential pressure, $P_T - P_s$, kPa
E	Young's Modulus of Elasticity, kPa
F_1	function defined in Equation 14 used in solution for fundamental frequency of stretched diaphram
F_2	function defined in Equation 14 used in solution for fundamental frequency of stretched diaphram
M	flow Mach number
P_A	ambient atmospheric pressure, kPa
P_N	percent non-linearity of diaphram deflection
P_q	dynamic pressure, $1/2\ \rho\ u^2$, kPa
P'_q	P_q calculated from Equation 4 using values of P_T and P_s multiplied by 1.03 or 0.97, kPa
P_s	side-on overpressure, kPa

P_T	stagnation overpressure, kPa
ΔP_s	magnitude of change in side-on overpressure, kPa
ΔP_T	magnitude of change in stagnation overpressure, kPa
R	diaphram radius, mm
R_N	ratio of terms in Equation 10 defining non-linearity of diaphram deflection
γ	ratio of specific heats (assumed to be 1.4)
ρ	air density, kg/m^3
ρ_d	density of diaphram material, kg/m^3
σ	Poisson's ratio
ω_m	mechanical fundamental frequency of diaphram, radians/s

DISTRIBUTION LIST

No. of Copies	Organization
12	Commander Defense Documentation Center ATTN: DDC-TCA Cameron Station Alexandria, VA 22314
3	Director Defense Advanced Research Projects Agency ATTN: Tech Lib NMRO PMO 1400 Wilson Boulevard Arlington, VA 22209
4	Director of Defense Research and Engineering ATTN: DD/TWP DD/S&SS DD/I&SS AD/SW Washington, DC 20301
1	Director Weapons Systems Evaluation Gp ATTN: Document Control Washington, DC 20305
1	Director Institute for Defense Analyses ATTN: IDA Librarian, Ruth S. Smith 400 Army-Navy Drive Arlington, VA 22202
2	Asst. to the Secretary of Defense (Atomic Energy) ATTN: Document Control Donald R. Cotter Washington, DC 20301
5	Director Defense Intelligence Agency ATTN: DT-IC DT-7D/E. O. Farrell DT-2/Wpns & Sys Div Technical Library DI-7E Washington, DC 20301
6	Director Defense Nuclear Agency ATTN: SPTD STSI/Archives SPAS/Mr. J. Moulton STSP STVL/Dr. La Vier RATN/Cdr Alderson Washington, DC 20305
6	Director Defense Nuclear Agency ATTN: DDST/Mr. P. Haas DDST/Mr. M. Atkins STTL/Tech Lib (2 cys) SPSS (2 cys) Washington, DC 20305
2	Commander Field Command, DNA ATTN: FCPR FCTMOF Kirtland AFB, NM 87115
1	Chief Las Vegas Liaison Office Field Command TD, DNA ATTN: Document Control P. O. Box 2702 Las Vegas, NV 89104
1	Commander Field Command, DNA Livermore Branch ATTN: FCPRL P. O. Box 808 Livermore, CA 94550

DISTRIBUTION LIST

No. of Copies	Organization
1	Director Defense Communications Agency ATTN: Code 930 Washington, DC 20305
3	Director Joint Strategic Target Planning Staff JCS ATTN: Sci & Tech Info Lib JLTW-2 DOXT Offutt AFB Omaha, NM 68113
1	Commander US Army Materiel Development and Readiness Command ATTN: DRCDMA-ST 5001 Eisenhower Avenue Alexandria, VA 22333
1	Commander US Army Materiel Development and Readiness Command ATTN: Technical Library 5001 Eisenhower Avenue Alexandria, VA 22333
1	Commander US Army Materiel Development and Readiness Command ATTN: W. H. Hubbard 5001 Eisenhower Avenue Alexandria, VA 22333
1	Commander US Army Aviation Research and Development Command ATTN: DRSAV-E 12th and Spruce Streets St. Louis, MO 63166
1	Director US Army Air Mobility Research and Development Laboratory Ames Research Center Moffett Field, CA 94035
5	Commander US Army Electronics Command ATTN: DRSEL-RD DRSEL-TL-IR R. Freiberg J. Roma A. Sigismondi E. T. Hunter Fort Monmouth, NJ 07703
1	Commander US Army Missile Research and Development Command ATTN: DRDMI-R Redstone Arsenal, AL 35809
3	Commander US Army Missile Materiel and Readiness Command ATTN: DRSMI-R DRSMI-XS, Ch Scientist Technical Library Redstone Arsenal, AL 35809
1	Commander US Army Tank Automotive Research & Development Cmd ATTN: DRDTA-RWL Warren, MI 48090

DISTRIBUTION LIST

No. of Copies	Organization
3	Commander US Army Mobility Equipment Research and Development Command ATTN: Tech Docu Cen, Bldg 315 DRSME-RZT DRXFB-RT, Dr. K. Oscar Fort Belvoir, VA 22060
1	Commander US Army Armament Materiel Readiness Command ATTN: DRSAR-LEP-L, Tech Lib Rock Island, IL 61299
3	Commander US Army Armament Research and Development Command ATTN: DRDAR-LCN P. Angelotti (2 cys) DRDAR-TSS Dover, NJ 07801
1	Commander US Army Armament Research and Development Command ATTN: DRDAR-LCN-F, Mr. Warren Reiner Dover, NJ 07801
1	Commander US Army Watervliet Arsenal Watervliet, NY 12189
5	Commander US Army Harry Diamond Lab ATTN: Mr. James Gaul Mr. L. Belliveau Mr. J. Gwaltney Mr. F. N. Wimenitz Mr. Bill Vault 2800 Powder Mill Road Adelphi, MD 20783
5	Commander US Army Harry Diamond Labs ATTN: DRXDO-TI DRXDO-TI/012 DRXDO-NP DRXDO-RBH Mr. P. A. Caldwell DELHD-RBA, J. Rosado 2800 Powder Mill Road Adelphi, MD 20783
3	Commander US Army Materials and Mechanics Research Center ATTN: Technical Library John Mescall Richard Shea Watertown, MA 02172
2	Commander US Army Natick Research and Development Command ATTN: DRXRE, Dr. D. Sieling DRXNM-UE Arthur Johnson Natick, MA 01762
1	Commander US Army Foreign Science and Technology Center ATTN: Rsch & Concepts Branch 220 7th Street, NE Charlottesville, VA 22901
2	Commander US Army Nuclear Agency ATTN: ACTA-NAW Technical Library 7500 Backlick Road, Bldg 2073 Springfield, VA 22150

DISTRIBUTION LIST

No. of Copies	Organization
2	Director US Army TRADOC Systems Analysis Activity ATTN: ATAA-SL (Tech Lib) LTC John Hesse White Sands Missile Range NM 88002
1	CDR, USA TRADOC ATTN: ATCD-SA/Mr. Oscar Wells Ft. Monroe, VA 23651
1	Interservice Nuclear Weapons School ATTN: Technical Library Kirtland AFB, NM 87115
2	HQDA (DAMA-AR; NCL Div) Washington, DC 20310
2	Office, Chief of Engineers Department of the Army ATTN: DAEN-MCE-D DAEN-RDM 890 South Pickett Street Alexandria, VA 22304
2	Deputy Chief of Staff for Operations and Plans ATTN: Technical Library Director of Chemical and Nuclear Operations Department of the Army Washington, DC 20310
2	Director US Army BMD Advanced Technology Center ATTN: CRDABH-X CRDABH-S Huntsville, AL 35807
1	Program Manager US Army BMD Program Office ATTN: John Shea 5001 Eisenhower Avenuye Arlington, VA 22333
1	Commander US Army BMD System Command ATTBL BDNSC-TFB/N. J. Hurst P. O. Box 1500 Huntsville, AL 35807
1	Commander US Army Research Office P. O. Box 12211 Research Triangle Park NC 27709
5	Commander US Army Engineer Waterways Experiment Station ATTN: Technical Library William Flathau John N. Strange Guy Jackson Leo Ingram P. O. 631 Vicksburg, MS 39180
2	Director Defense Civil Preparedness Agency ATTN: Mr. George Sisson/RF-SR Technical Library Washington, DC 20301
1	Commander US Army Engineering Center ATTN: ATSEN-SY-L Fort Belvoir, VA 22060
1	Division Engineer US Army Engineering Division Ohio River ATTN: Docu Cen P. O. Box 1159 Cincinnati, OH 45201

DISTRIBUTION LIST

No. of Copies	Organization
1	Division Engineer US Army Engineering Division ATTN: HNDSE-R/M. M. Dembo Huntsville Box 1600 Huntsville, AL 35804
1	Commander Combined Arms Combat Developments Activity ATTN: ATCA-CO/Mr. L. C. Pleger Ft. Leavenworth, KS 66027
1	Commander US Army Logistical Center ATTN: ATCL-SCA/Mr. Robert Cameron Ft. Lee, VA 23801
4	Office of Naval Research ATTN: Code 461/Jacob L. Warner Code 461/Thomas P. Quinn N. Perrone 800 N. Quincy Street Arlington, VA 22217
2	Chief of Naval Operations ATTN: OP-03EG OP-985F Department of the Navy Washington, DC 20350
1	Chief of Naval Material ATTN: MAT 0323 Department of the Navy Arlington, VA 22217
3	Director Strategic Systems Projects Ofc ATTN: NSP-43, Tech Lib NSP-273 NSP-272 Department of the Navy Washington, DC 20360
1	Commander Naval Electronic Systems Com ATTN: PME 117-21A Washington, DC 20360
2	Commander Naval Sea Systems Command ATTN: ORD-91313 Library Code 03511 Department of the Navy Washington, DC 20362
3	Commander US Naval Facilities Engineering Command ATTN: Code 03A Code 04B Technical Library Washington, DC 20360
4	Officer-in-Charge Civil Engineering Laboratory Naval Constr Btn Ctr ATTN: Stan Takahashi R. J. Odello John Crawford Technical Library Port Hueneme, CA 93041
2	Commander Naval Ship Engineering Center ATTN: Technical Library NSEC 6105G Hyattsville, MD 20782
1	Commander David W. Taylor Naval Ship Research & Development Center ATTN: L42-3 Library Bethesda, MD 20084

DISTRIBUTION LIST

No. of Copies	Organization
3	Commander US Naval Surface Weapons Center ATTN: Code WA501/Navy Nuclear Programs Office Code WX21/Tech Lib Code 240/C. J. Aronson Silver Spring, MD 20910
1	Commander US Naval Surface Weapons Center ATTN: DX-21, Library Br. Dahlgren, VA 22448
2	Commander US Naval Ship Research and Development Center Facility Underwater Explosions Research Division ATTN: Code 17/W. W. Murray Technical Library Portsmouth, VA 23709
1	Commander US Naval Weapons Center ATTN: Code 533/Tech Lib China Lake, CA 93555
2	Commander US Naval Weapons Evaluation Facility ATTN: Document Control R. Hughes Kirtland AFB Albuquerque, NM 87117
2	Commander US Naval Research Laboratory ATTN: Code 2027/Tech Lib Code 8440/F. Rosenthal Washington, DC 20375
1	Superintendent US Naval Postgraduate School ATTN: Code 2124/Tech Rpts Lib Monterey, CA 93940
1	HQ USAF (IN) Washington, DC 20330
1	HQ USAF (PRE) Washington, DC 20330
2	AFSC (DLCAW; Tech Lib) Andrews AFB Washington, DC 20331
2	AFATL (ATRD/R. Brandt) Eglin AFB, FL 32542
2	ADTC (ADBRL-2; Tech Lib) Eglin AFB, Florida 32542
2	RADC (EMTLD/Docu Lib; EMREC/ R. W. Mair) Griffiss AFB, NY 13340
1	AFWL/SUL Kirtland AFB, NM 87117
1	AFWL/DE-I Kirtland AFB, NM 87117
1	AFWL/DEX Kirtland AFB, NM 87117
1	AFWL/Robert Port Kirtland AFB, NM 87117
1	AFWL/DEV Jimmie L. Bratton Kirtland AFB, NM 87117
1	AFWL/R. Henny Kirtland AFB, NM 87117
1	AFWL/DEV M. A. Plamondon Kirtland AFB, NM 87117
2	Commander-in-Chief Strategic Air Command ATTN: NRI-STINFO Lib XPFS Offut AFB, NB 68113

DISTRIBUTION LIST

No. of Copies	Organization
1	AFML (MAMD/Dr. T. Nicholas) Wright-Patterson AFB OH 45433
4	FTD (TDFBD; TDPMG; ETET/ CAPT R. C. Husemann; TD-BTA/Lib) Wright-Patterson AFB OH 45433
1	ASD (Tech Lib) Wright-Patterson AFB OH 45433
2	ADC (XP; XPQDQ) Wright-Patterson AFB OH 45433
1	AFIT (Lib Bldg. 640, Area B) Wright-Patterson AFB OH 45433
1	Director US Bureau of Mines ATTN: Technical Library Denver Federal Center Denver, CO 80225
1	Director US Bureau of Mines Twin Cities Research Center ATTN: Technical Library P. O. Box 1660 Minneapolis, NM 55111
1	US Energy Research and Development Administration Division of Headquarters Svcs ATTN: Doc Control for Classified Tech Lib Library Branch G-043 Washington, DC 20545
1	US Energy Research and Development Administration Albuquerque Operations Office ATTN: Doc Control for Tech Lib P. O. Box 5400 Albuquerque, NM 87115
1	US Energy Research and Development Administration Nevada Operations Office ATTN: Doc Control for Tech Lib P. O. Box 14100 Las Vegas, NV 89114
5	Director Lawrence Livermore Laboratory ATTN: L. W. Woodruft/L-96 Tech Info Dept L-3 D. M. Norris/L-90 Ted Butkovich/L-200 J. R. Hearst/L-205 P. O. Box 808 Livermore, CA 94550
4	Director Lawrence Livermore Laboratory ATTN: Jack Kahn/L-7 J. Carothers/L-7 Robert Schock/L-437 R. G. Dong/L-90 P. O. Box 808 Livermore, CA 94550
4	Director Los Alamos Scientific Laboratory ATTN: Doc Control for Rpts Lib R. A. Gentry G. R. Spillman Al Davis P. O. Box 1663 Los Alamos, NM 87544

DITRIBUTION LIST

No. of Copies	Organization
1	Director National Aeronautics and Space Administration Scientific and Technical Information Facility P. O. Box 8757 Baltimore/Washington International Airport, MD 21240
3	Aerospace Corporation ATTN: Tech Info Services (2 cys) P. N. Mathur P. O. Box 92957 Los Angeles, CA 90009
1	Agbabian Associates ATTN: M. Agbabian 250 North Nash Street El Segundo, CA 90245
1	Analytic Services, Inc. ATTN: George Hesselracher 5613 Leesburg Pike Falls Church, VA 22041
1	Applied Theory, Inc. ATTN: John G. Trulio 1010 Westwood Blvd. Los Angeles,CA 90024
1	Artec Associates, Inc. ATTN: Steven Gill 26046 Eden Landing Road Hayward, CA 94545
1	AVCO ATTN: Res Lib A830, Rm 7201 201 Lowell Street Wilmington, MA 01887
2	The BDM Corporation ATTN: Technical Library A. Lavagnino 1920 Aline Avenue Vienna, VA 22180
1	The BDM Corporation ATTN: Richard Hensley P. O. Box 9274 Albuquerque International Albuquerque, NM 87119
2	The Boeing Company ATTN: Aerospace Library R. H. Carlson P. O. Box 3707 Seattle, WA 98124
1	Brown Engineering Co., Inc. ATTN: Manu Patel Cummings Research Park Huntsville, AL 35807
2	California Research and Technology, Inc. ATTN: Ken Kreyenhagen Technical Library 6269 Variel Avenue Woodland Hills, CA 91364
1	Calspan Corporation ATTN: Technical Library P. O. Box 235 Buffalo, NY 14221
1	Civil/Nuclear Systems Corporation ATTN: Robert Crawford 1200 University N. E. Albuquerque, NM 87102
1	EG&G, Incorporated Albuquerque Division ATTN: Technical Library P. O. Box 10218 Albuquerque, NM 87114
1	The Franklin Institute ATTN: Zemons Zudans 20th Street and Parkway Philadelphia, PA 19103

DISTRIBUTION LIST

No. of Copies	Organization
1	General American Trans Corporation General American Research Division ATTN: G. L. Neidhardt 7449 N. Natchez Avenue Niles, IL 60648
1	General Electric Company-TEMPO ATTN: DASIAC P. O. Drawer QQ Santa Barbara, CA 93102
1	General Research Corporation ATTN: Benjamin Alexander P. O. Box 3587 Santa Barbarba, CA 93105
2	Hazeltine Corp ATTN: Carl Meinen Greenlawn, NY 11740
1	J. H. Wiggins Co., Inc. ATTN: John Collins 1650 South Pacific Cost Highway Redondo Beach, CA 90277
6	Kaman Avidyne ATTN: Dr. N. P. Hobbs (4 cys) Mr. S. Criscione Mr. John Calligeros 83 Second Avenue Northwest Industrial Park Burlington, MA 01830
3	Kaman Sciences Corporation ATTN: Library P. A. Ellis F. H. Shelton 1500 Garden of the Gods Road Colorado Springs, CO 80907
1	Lockheed Missiles & Space Co. ATTN: Technical Library P. O. Box 504 Sunnyvale, CA 94088
2	Martin Marietta Aerospace Orlando Division ATTN: G. Fotieo Mail Point 505, Craig Luongo P. O. Box 5837 Orlando, FL 32805
3	McDonnell Douglas Astronautics Corporation ATTN: Robert W. Halprin Mr. C. Gardiner Dr. P. Lewis 5301 Balsa Avenue Huntington Beach, CA 92647
2	Merritt Cases, Inc. ATTN: J. L. Merritt Technical Library P. O. Box 1206 Redlands, CA 92373
1	Meteorology Research, Inc. ATTN: W. D. Green 464 West Woodbury Road Altadena, CA 91001
1	The Mitre Corporation ATTN: Library P. O. Box 208 Bedford, MA 01730
2	Pacifica Technology ATTN: G. Kent R. Bjork P. O. Box 148 Del Mar, CA 92014

DISTRIBUTION LIST

No. of Copies	Organization
4	Physics International Corp. ATTN: E. T. Moore Dennis Orphal Coye Vincent F. M. Sauer 2700 Merced Street San Leandro, CA 94577
4	Physics International Corp ATTN: Robert Swift Charles Godfrey Larry A. Behramann Technical Library 2700 Merced Street San Leandro, CA 94577
5	R&D Associates ATTN: Dr. H. L. Brode Dr. Albert L. Latter C. P. Knowles William B. Wright Henry Cooper P. O. Box 9695 Marina del Rey, CA 90291
4	R&D Associates ATTN: Jerry Carpenter Sheldon Schuster J. G. Lewis Technical Library P. O. Box 9695 Marina del Rey, CA 90291
1	The Rand Corporation ATTN: C. C. Mow 1700 Main Street Santa Monica, CA 90406
6	Sandia Laboratories ATTN: Doc Control for 3141 Sandia Rpt Collection A. J. Chaban M. L. Merritt L. J. Vortman W. Roherty L. Hill P. O. Box 5800 Albuquerque, NM 87115
1	Sandia Laboratories Livermore Laboratory ATTN: Doc Control for Tech Lib P. O. Box 969 Livermore, CA 94550
1	Science Applications, Inc. ATTN: Technical Library P. O. Box 3507 Albuquerque, NM 87110
2	Science Applications, Inc. ATTN: R. Seebaugh John Mansfield 1651 Old Meadow Road McLean, VA 22101
1	Science Applications, Inc. 8201 Capwell Drive Oakland, CA 94621
2	Science Applications, Inc. ATTN: Technical Library Michael McKay P. O. Box 2351 La Jolla, CA 92038
4	Systems, Science & Software ATTN: Donald R. Grine Ted Cherry Thomas D. Riney Technical Library P. O. Box 1620 La Jolla, CA 92037

DISTRIBUTION LIST

No. of Copies	Organization
3	Terra Tek, Inc. ATTN: Sidney Green Technical Library A. H. Jones 420 Wakara Way Salt Lake City, UT 84108
2	Tetra Tech, Inc. ATTN: Li-San Hwang Technical Library 630 North Rosemead Blvd. Pasadena, CA 91107
7	TRW Systems Group ATTN: Paul Lieberman Benjamin Sussholtz Norm Lipner William Rowan Jack Farrell Pravin Bhutta Tech Info Ctr/S-1930 One Space Park Redondo Beach, CA 90278
1	TRW Systems Group ATTN: Greg Hulcher San Bernardino Operations P. O. Box 1310 San Bernardino, CA 92402
2	Union Carbide Corporation Holifield National Laboratory ATTN: Doc Control for Tech Lib Civil Defense Research Proj P. O. Box X Oak Ridge, TN 37830
1	Universal Analytics, Inc. ATTN: E. I. Field 7740 W. Manchester Blvd. Playa del Rey, CA 90291
1	Weidlinger Assoc. Consulting Engineers ATTN: M. L. Baron 110 East 59th Street New York, NY 10022
1	Westinghouse Electric Company Marine Division ATTN: W. A. Votz Hendy Avenue Sunnyvale, CA 94008
2	Battelle Memorial Institute ATTN: Technical Library R. W. Klingesmith 505 King Avenue Columbus, OH 43201
1	California Institute of Technology ATTN: T. J. Ahrens 1201 E. California Blvd. Pasadena, CA 91109
2	COSMIC ATTN: L. C. Gadol 112 Barrow Hall University of Georgia Athens, GA 30602
2	Denver Research Institute University of Denver ATTN: Mr. J. Wisotski Technical Library P. O. Box 10127 Denver, CO 80210
3	IIT Research Institute ATTN: Milton R. Johnson R. E. Welch Technical Library 10 West 35th Street Chicago, IL 60616

DISTRIBUTION LIST

No. of Copies	Organization
2	Lovelace Foundation for Medical Education ATTN: Asst. Dir. of Research/ Robert K. Jones Technical Library 5200 Gibson Blvd, SE Albuquerque, NM 87108
1	Massachusetts Institute of Technology Aeroelastic and Structures Research Laboratory ATTN: Dr. E. A. Witmer Cambridge, MA 02139
2	Southwest Research Institute ATTN: Dr. W. E. Baker A. B. Wenzel 8500 Culebra Road San Antonio, TX 78206
2	Stanford Research Institute ATTN: Dr. G. R. Abrahamson Carl Peterson 333 Ravenswood Avenue Menlo Park, CA 94025
1	University of Dayton Industrial Security Super. KL-505 ATTN: H. F. Swift 300 College Park Avenue Dayton, OH 45409
1	University of Illinois Consulting Engineering Services ATTN: Nathan M. Newmark 1211 Civil Engineering Building Urbana, IL 61801
2	The University of New Mexico The Eric H. Wang Civil Engineering Research Facility ATTN: Larry Bickle Neal Baum University Station Box 188 Albuquerque, NM 87131
2	Washington State University Administration Office ATTN: Arthur Miles Hohorf George Duval Pullman, WA 99163
	Aberdeen Proving Ground
	Marine Corps Ln Ofc Dir, USAMSAA ATTN: Dr. J. Sperrazza Mr. R. Norman, GWD